CSCE Annual Conference

Growing with youth – Croître avec les jeunes

Laval (Greater Montreal)

June 12 - 15, 2019

EFFECT OF SHEAR SPAN-TO-DEPTH RATIO ON THE SEISMIC PERFORMANCE OF REINFORCED CONCRETE MASONRY STRUCTURAL WALLS WITH BOUNDARY ELEMENTS

Aly, N.[1] and Galal, K.[2]

[1] Ph.D. Candidate, Department of Building, Civil and Environmental Engineering, Concordia University, Montréal, Québec, Canada, n_aly@encs.concordia.ca

[2] Professor, Department of Building, Civil and Environmental Engineering, Concordia University, Montréal, Québec, Canada, khaled.galal@concordia.ca

Abstract: Reinforced Concrete Masonry (RCM) is a competitive alternative construction material for buildings. In the 2015 edition of the National Building Code of Canada (NBCC-2015) a ductile category of RCM shear walls was added. The ductile response could be achieved in RCM shear walls by integrating confined masonry boundary elements to the ends of the rectangular walls. Majority of the tested RCM shear walls with boundary elements represented walls in low- to mid-rise buildings. Thus, the intent of this study is to investigate the structural performance of high-rise ductile RCM structural walls with boundary elements under reversed cyclic loading simulating seismic actions. This is achieved by testing two half-scale fully grouted RCM shear walls with boundary elements under quasi-static reversed cyclic loading and constant axial load. The walls were designed and constructed with similar geometry and material properties and were tested under the same level of axial stress. The main parameter investigated in this study is the shear span-to-depth ratio. The tested specimens represented the plastic hinge regions of shear walls in 6-story and 12-story RCM buildings. The results confirmed the capability of the presence of sufficiently confined boundary elements in providing a ductile response for the walls with high aspect ratios. The reduction in the aspect ratio (from 6-story to 12-story) triggered a higher contribution from the shear mechanisms and increased the rate of cyclic strength degradation. The normalized response of the two walls demonstrated the limited influence of the changes in height relative to the impact of changes in the cross-section configuration.

1 INTRODUCTION

In Canada, unreinforced masonry has been extensively utilized in low-rise buildings located in low seismic hazard regions. Conversely, Reinforced Concrete Masonry (RCM) was used in mid- and high-rise buildings, but also in regions with low seismicity (Drysdale and Hamid 2005). For example, the 24-story apartment building (Place Louis Riel) in Winnipeg (Drysdale and Hamid 2005) and the 20-story building in Brazil (Correa 2016). With the evolution of building codes and design standards, the use of unreinforced masonry became very limited and more demand was shifted towards RCM structural systems. RCM compared to other construction materials presents a competitive alternative with relatively rapid construction and reasonably built-in soundproofing and fire insulation characteristics. The most common Seismic Force Resisting System (SFRS) in masonry buildings is RCM structural walls. A ductile category of RCM shear walls was added in the 2015 edition of the National Building Code of Canada (NBCC-15). The Canadian masonry design standard (i.e. CSA S304-14) assigned special design and detailing requirements to the

ductile walls to ensure a stable ductile response and to qualify for a higher ductility-related response modification factor (R_d) of 3.0. The higher ductility-related response modification factor (R_d) would result in reduced seismic design forces and more competitive designs. In RCM shear walls, the ductile response is best achieved by integrating confined masonry boundary elements at the ends of the rectangular walls. Majority of the tested RCM shear walls with boundary elements represented walls in 2- to 3-story masonry buildings (Banting and El-Dakhakhni 2014; Shedid et al. 2010). Up to the authors' knowledge, there is a limited number of studies that investigated the cyclic response of high-rise RCM structural walls.

Ahmadi et al. (2014) tested 30 grouted RCM shear walls under reversed cyclic loading. The aim was to establish the trends between important design parameters, such as aspect ratio, axial load level, vertical reinforcement ratio, configuration and lap splices and the nonlinear load-displacement response of the walls. The authors highlighted that the ratio between the measured lateral capacity and estimated nominal resistance marginally decreased with the increase in axial load. However, there was no clear impact from neither aspect ratio nor the ratio of vertical reinforcement. The maximum lateral drifts (measured at 20% strength degradation) varied from 0.9% to 4.51% for the tested walls. Maximum drifts were not affected by axial load level but increased with the increase in aspect ratio and vertical reinforcement ratio. The measured displacement ductility for the walls was ranging between 2.8 to 11.04 and was not influenced by aspect ratio or axial load level. Nevertheless, the increase in vertical reinforcement ratio clearly decreased the displacement ductility of the tested walls. The experimentally measured plastic hinge length of the tested walls ranged from 10% to 41%. It was noted that plastic hinge length was not significantly affected by vertical reinforcement ratio, however, it increased with the increase in axial load and aspect ratio. The authors concluded that the decrease in aspect ratio increases the initial stiffness, flexural capacity and the rate of strength degradation. Conversely, it decreases the ultimate drift ratio of the walls. Likewise, based on their experimental results, they noted that increasing the axial load increased the initial stiffness, reduced lateral drift at failure and increased the strength degradation. The increase in vertical reinforcement ratio also increased initial stiffness and reduced the maximum lateral drift.

Banting and El-Dakhakhni (2014) tested five half-scale RM walls with boundary elements having varying heights, lengths and vertical reinforcement ratios. The objective was to prove that the compressive strain of masonry can be increased with confinement. Based on their experimental results, it was concluded that the force-based response of the walls was highly dependent on the horizontal extent of boundary elements. Besides, the increase in the walls' aspect ratios resulted in increasing the experimentally measured plastic hinge length, curvature ductility, and displacement ductility. The results also suggested that an increase in vertical reinforcement ratio would adversely affect the displacement ductility of the wall. Furthermore, it was recommended to account for shear deformations in design, as it had a major contribution to the walls' structural response. It was concluded that the presence of confined masonry boundary elements substantially improved the overall response of RM shear walls.

It is evident from the literature that there is a great potential for ductile RCM with boundary elements as a competitive alternative SFRS in mid- and high-rise buildings. However, there is a need for more testing to explore the design challenges and investigate the stability of the nonlinear response for walls with higher aspect ratios. Thus, this paper aims to present the experimental testing of two half-scale RCM shear walls with boundary elements. The tested specimens are panels simulating the plastic hinge region of shear walls in 12-story and 6-story typical RCM buildings. The objective is to asses the structural performance of high-rise RCM masonry shear walls with boundary elements and to quantify the influence of the shear span-to-depth ratio on the structural response.

2 EXPERIMENTAL SPECIMENS

In this study, two half-scale RCM shear walls (W1 and W2) with boundary elements were tested under constant axial load and displacement-controlled quasi-static reversed cyclic loading to simulate the response under seismic excitations. Due to the limitations involved in handling and testing full large-scale specimens, only the plastic hinge regions were tested. The two tested wall panels represented a conservative estimate of the plastic hinge region of a 12-story and 6-story prototype buildings. The prototype buildings were assumed to have a first-floor height of 3.2m and a typical floor height of 3m, thus

a total full-scale height of 36.2m and 18.2m for the 12-story and 6-story buildings, respectively. The corresponding half-scale heights are 18.1m for the 12-story building and 9.1m for the 6-story building. The tested specimens were 2.38m high with an out-of-plane support system placed at 1.6m to represent the first-floor slab. In addition, out-of-plane displacements were restrained at the location of the load application. The two walls had the same cross-sectional dimensions and reinforcement details shown in Figure 1. Furthermore, the specimens were tested under the same axial pre-compression stress of 2.25MPa. The axial pre-compression load level was selected to result in an axial load ratio ($P/A_g f'_m$) higher than 10% and compression zone depths extending beyond the boundary elements at ultimate loads.

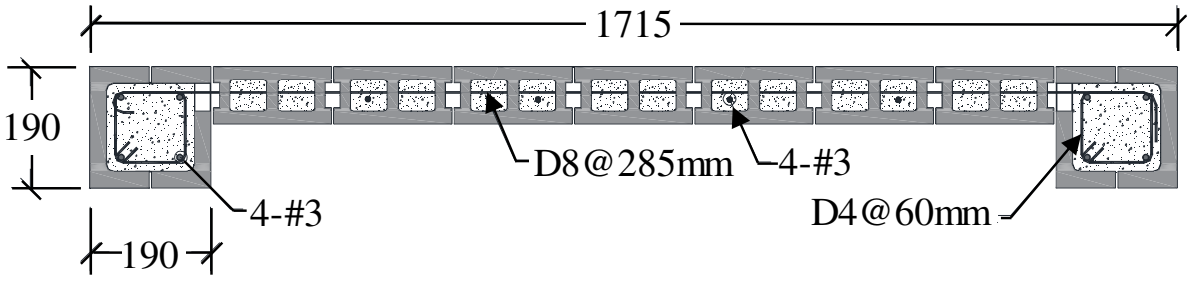

Figure 1: Cross-section of tested walls (all dimensions are in mm)

It is acknowledged that the axial pre-compression load is expected to be lower on the shorter wall if the two buildings are assumed to have the same layout. However, it is possible for the 12-story and 6-story walls to have similar axial compressive loads assuming that the buildings had different layout and spans. This was essential to quantify the influence of the shear span-to-depth ratio (M/Vd_v) on the cyclic response and isolate other parameters. The only difference between the two tested specimens was the shear span-to-depth ratio (M/Vd_v). The first specimen (W1) represented a 12-story wall and had a shear span-to-depth ratio of 8.8 while W2 represented a 6-story wall with M/Vd_v of 4.4. The two walls were designed and detailed following the requirements of CSA S304-14 to ensure a flexural dominated response. In addition, the specimens were constructed by the same professional mason in the structures laboratory at Concordia University. A half-scale version of the standard 190mm concrete stretcher blocks was used to build the walls' web in a running bond pattern with 5mm of Type-S mortar joints. The half-scale stretcher units had the dimensions of 185mm x 90mm x 90mm. For the walls' boundary elements, C-shaped concrete blocks were cut from pilaster units to form the required dimensions (i.e. 190mmx190mm). The C-shaped blocks were laid in a stack pattern with 5mm Type-S mortar joints. The walls' webs were grouted using an ordinary strength fine grout, whereas a high strength fine grout was used in grouting the boundary elements.

2.1 Material Properties

As the two specimens (W1 and W2) were constructed in two phases, material samples were taken during the construction of each wall. The average compressive strength of the boundary elements blocks was 22.8 MPa (c.o.v. = 4.8%) and 27.6 MPa (c.o.v. = 5.6%) for walls W1 and W2, respectively. The C-shaped blocks were sampled and tested according to ASTM C140-15 by taking coupons with height to thickness ratio of 2 and length to thickness ratio of 4. The walls' web and boundary elements were joined using a 5 mm joint of pre-mixed Type-S mortar. The mortar cube specimens taken during the construction of both walls had an average compressive strength of 15 MPa. The average cylinder compressive strength of the ordinary strength fine grout was 31.3 MPa (c.o.v. = 9.5%) for wall W1 and 31 MPa (c.o.v. = 11.1%) for wall W2. The high strength fine grout was 43.2 MPa (c.o.v.= 15.5%) and 42.6 MPa (c.o.v. = 5.6%) for walls W1 and W2, respectively. The mortar cubes and grout cylinders were sampled and tested in accordance with CSA A179-14. From each construction phase, 4-blocks high by 1-block long prisms and 4-courses high prisms of C-shaped blocks forming the square 190 mm x 190 mm boundary elements were tested under concentric compression according to CSA S304-14 to evaluate the masonry compressive strength (f_m). The prisms of the walls' webs were grouted using the ordinary strength grout, and the boundary element prims were grouted using the high strength grout. The average web compressive strength (f_m) was 10.3 MPa (c.o.v. =

3%) for wall W1 and 14.6 MPa (c.o.v. = 3%) for wall W2. The boundary elements average compressive strength (f_m) was 21.8 MPa (c.o.v. = 9%) and 23.2 MPa (c.o.v. = 16%) for walls W1 and W2, respectively. It should be noted that the reported average compressive strengths for the prisms were corrected to account for the height-to-thickness ratios as required by Annex D of CSA S304-14. The vertical reinforcing rebars (No. 3, cross-section area of 71 mm^2) used in the walls had an average yield strength of 460 MPa.

2.2 Test Setup and Testing Scheme

The walls were tested under a constant axial compressive load and reversed cyclic loading until failure. Since the walls represented the expected plastic hinge regions and not the full specimen, a moment was applied on the top of the tested walls to compensate for the difference in height between the full specimen and the tested panel. The test setup and the externally mounted instrumentations are illustrated in Figure 2.

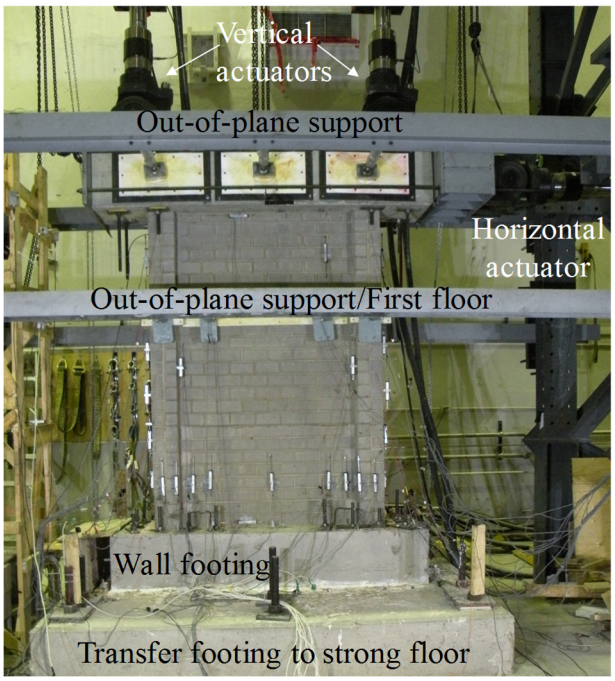

Figure 2: Experimental test setup and external instrumentation

The walls were first subjected to the constant axial pre-compression stress in a force-controlled mode using the two vertical actuators. Then, using the horizontal actuator, fully-reversed cycles of lateral displacements were applied following the loading protocol shown in Figure 3. The loading protocol consisted of increments and multipliers of a representative damage state as recommended by Federal Emergency Management Agency (FEMA 461-2007). In the present study, the first yield in the vertical reinforcement at the wall-foundation interface was selected as the damage state. Thus, the lateral displacement corresponding to the first yield was used to form the loading protocol. The first yield displacement was captured using internally mounted strain gauges on the two outermost vertical rebars in the boundary elements. The walls were cycled twice at each lateral displacement level to capture the cyclic and in-cycle degradation in strength and stiffness. At each displacement cycle, the horizontal resistance, measured by the horizontal actuator load-cell, was used to calculate the corresponding top moment to be applied by the vertical actuators. The two vertical actuators were used to apply the axial compressive force in addition to the coupled forces required to induce the corresponding top moment. A triangular load distribution was assumed for calculating the walls' effective height to conform with the NBCC-15 equivalent static force analysis method. To capture the post-peak response, the lateral displacements were gradually increased, as multiples of the yield displacement, until 20% degradation in the peak strength or until the wall was

incapable of sustaining the applied vertical load which simulated the gravity loads. In testing, the difference in the shear span-to-depth ratio (M/Vd_v) between W1 and W2 was accounted for by the applied top moment. As such, specimen W2 which represented the 6-story ($M/Vd_v = 4.4$) wall had a lower top moment compared to the 12-story wall (i.e. W1 with $M/Vd_v = 8.8$).

The specimens were internally instrumented with 20 5-mm strain gauges to capture the first yield, measure the extent of strain penetration into the wall footing and the extent of yielding over the wall height. Additionally, Linear Variable Displacement Transducers (LVDTs) and linear potentiometers were externally attached to the walls. LVDTs were used to measure the vertical displacements and monitor any sliding or uplift displacements at the wall-foundation interfaces. The linear potentiometers were used to measure the lateral displacements from an independent reference and measure the diagonal shear deformations. Furthermore, linear potentiometers were used to monitor any sliding or uplift displacements between the wall footing and the transfer footing to the strong floor.

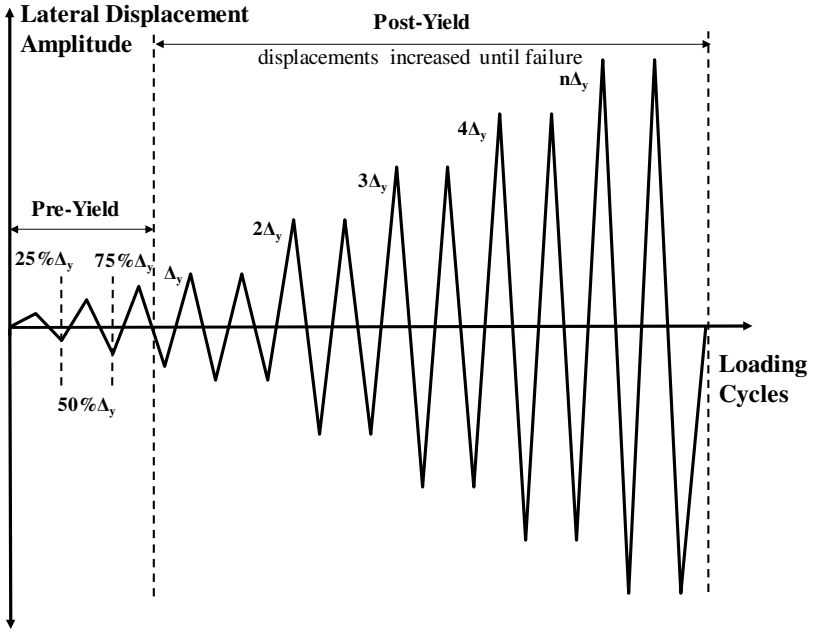

Figure 3: Loading protocol

3 RESULTS

3.1 Load-Displacement Response

The hysteretic response envelopes of walls W1 and W2 are shown in Figure 4. It should be noted that the lateral resistance measured by the horizontal actuator was corrected to account for the horizontal component from the two vertical actuators, especially at high lateral displacements. As seen in Figure 4, the response of walls W1 and W2 was linear elastic during the pre-yield stage of the loading protocol. The initial secant stiffness, at the lateral displacement of $0.25\Delta_y$, is almost 4.3 higher for the 6-story wall (W2) in comparison with the 12-story wall (W1). There was an apparent reduction in the lateral secant stiffness after the initial loading cycle of $0.25\Delta_y$. The changes in the lateral stiffness were lesser for the remaining pre-yield cycles. At the lateral displacement corresponding to the first yield (Δ_y), a significant drop in the lateral stiffness was seen in the response of both specimens. The lateral stiffness at yield dropped by 47% for W1 and 77% for W2 from the initial secant stiffness at $0.25\Delta_y$. Both walls exhibited a symmetric cyclic response. The lateral loads at first yield were very similar between the push and pull directions. Additionally, marginal differences were noticed between peak loads in the two directions. This demonstrates that the

walls had a uniform cross-section without any cavities or voids in the grouted cells. Furthermore, both walls displayed a ductile response reflected in the ability of the walls to reach large inelastic lateral deformation, beyond the elastic range, without substantial reduction in its load carrying capacities. The average ratio between the ultimate and yield lateral loads for W1, the plastic hinge region of a 12-story wall, was 1.27. Conversely, a lower ratio of 1.16 between the ultimate and yield loads was observed in the response of wall W2 which represented the plastic hinge region of a 6-story wall. This could be attributed to the influence of the reduction in the shear span-to-depth ratio on increasing the contribution of shear deformations to the overall cyclic response. As a result, there was no significant strain-hardening in the reinforcement of the 6-story wall (i.e. W2). Furthermore, as shown in Figure 4, W2 had more distinct progressive degradation in strength compared to W1. Unlike wall W1, the spalling of the boundary elements' blocks face-shell resulted in a drop in the lateral resistance of wall W2. Wall W1 had a stable and a hardening cyclic response until the wall was incapable of sustaining the applied compressive vertical load.

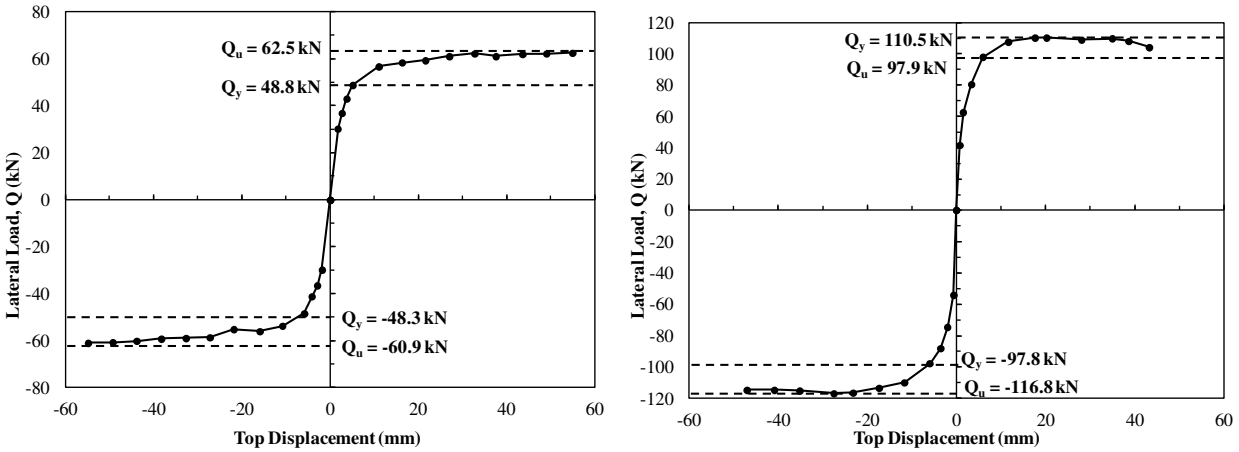

Figure 4: Load-displacement envelopes: (a) Wall W1; (b) Wall W2

The interaction between the flexure and shear responses was evident in the ultimate displacement capacity of wall W2. Both walls had an identical cross-section with similar material properties; however, W2 exhibited a limited ultimate displacement capacity compared to W1. Walls W1 and W2 had similar first yield displacements, measured at the top of tested specimens, of 5.6mm and 6mm, respectively. However, the yield displacement at the top of wall W2 is expected to be lesser than W1 due to the difference in shear span-to-depth ratios. Wall W1 reached its failure criteria at the top of tested wall displacement equal to 56mm, which corresponds to 2.35% drift at the top of the tested specimen. On the other hand, W2 failed at a top displacement of 48mm which corresponds to a top of wall drift equal to 2.02%. Thus, wall W1 failed at a displacement-ductility (μ_Δ) of 10, while wall W2 failed at a displacement-ductility (μ_Δ) of 8. The displacement ductility was calculated as the ratio between the ultimate displacement, measured at either 20% strength degradation or when the wall was incapable of sustaining the vertical load, and the experimentally measured first yield displacement. It is interesting to highlight that for the 12-story wall, the failure was due to the inability of the wall to sustain the applied vertical loads which simulated the gravity loads. This is mainly attributable to the high rotation at the top of the tested specimen. Conversely, the 6-story wall had a distinct degradation in lateral resistance before its failure due to the reduced top rotation relative to W1. Thus, it was possible to terminate the test when the degradation exceeded 20% from the peak load.

Figure 5 presents the normalized envelopes of walls W1 and W2. The lateral load (Q) is normalized by probable lateral resistance (Q_p) calculated using the flexural strength equations of CSA S304-14. The actual material properties were used without the material strength reduction factors (Φ_m and Φ_s) and accounting for the reinforcement strain-hardening. The strain-hardening was considered by using a factor of 1.25 to

account for the difference between the yield strength and the probable strength of the reinforcing steel. This factor is commonly used in the capacity design by the majority of international design standards. The top of wall displacement is normalized by the height of the tested specimen. It can be seen that both walls exhibited an almost identical response until the first yield. In the post-yield stage, the 12-story wall (W1) had a hardening response until failure; nevertheless, the 6-story wall (W2) had a degrading post-peak response. For the 12-story wall (W1) there was a 95% match between the predicted probable resistance (Q_p) and the peak experimental resistance. However, the peak resistance of the 6-story wall (W2) was overestimated by 14%. This confirms the limited contribution from the strain-hardening of the vertical reinforcement to the ultimate resistance and the increased contribution from the shear mechanism in the 6-story wall. The wall with the smaller shear span-to-depth ratio did not achieve the assumed 25% increase in the reinforcing steel strength due to the increased contribution from shear deformations. As discussed in the previous subsection, the strain-hardening was 27% for W1 and 16% for W2.

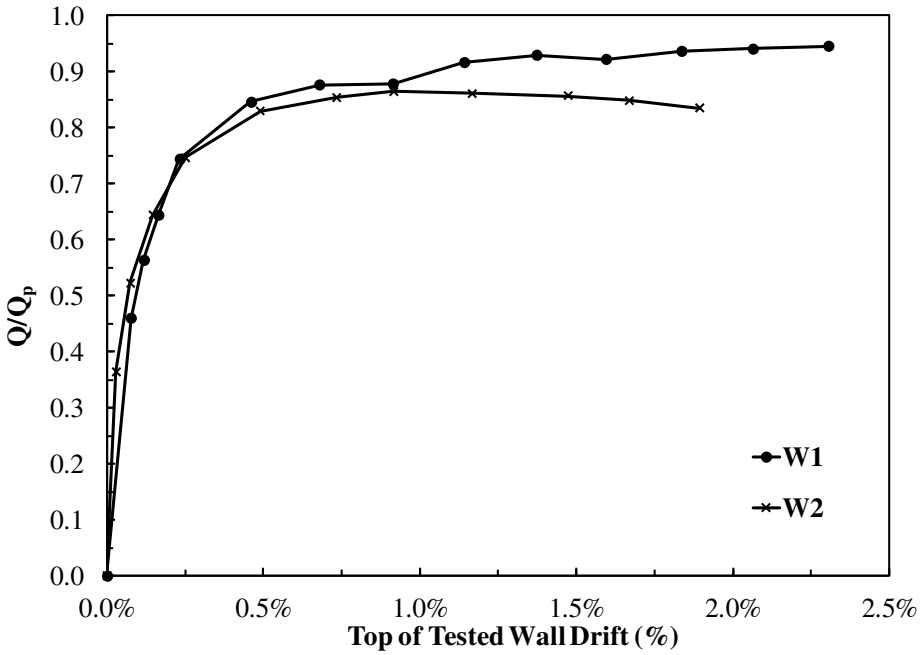

Figure 5: Normalized load-displacement envelopes

The normalized response shown in Figure 5 reflects an overall similar cyclic response for the two specimens. This demonstrates that the overall performance of structural walls is more dependent on the walls' cross-section compared to its height. This is also reflected in most plastic hinge height predication equations, including the equation of CSA S304-14 for ductile RCM shear walls, which denote a limited contribution of 10% to the wall height. This is in line with the findings of other studies, such as (Shedid et al. 2010). However, it is evident that the reduction in the shear span-to-depth ratio increases the initial stiffness, the rate of stiffness deterioration, the strength degradation and the contribution of the shear to the overall response. Furthermore, it limits the ultimate displacement capacity and thus reduces the wall displacement-ductility.

3.2 Damage State

Figure 6 presents the final damage state and the cracking pattern of walls W1 and W2. Both walls had hairline horizontal cracks in the mortar bed joints after the first cycle to the first yield lateral displacement (Δ_y). In addition, the 6-story wall (W2) had the first shear step crack at the lateral displacement level of Δ_y. On the other hand, the 12-story wall (W1) had the first diagonal shear crack after the second cycle to the displacement level of $5\Delta_y$ and only a few shear cracks were observed afterwards until failure. W2 had a

more distinct damage progression that had an evident influence on its load-displacement response, whereas the damage in W1 had a lesser impact on the lateral resistance.

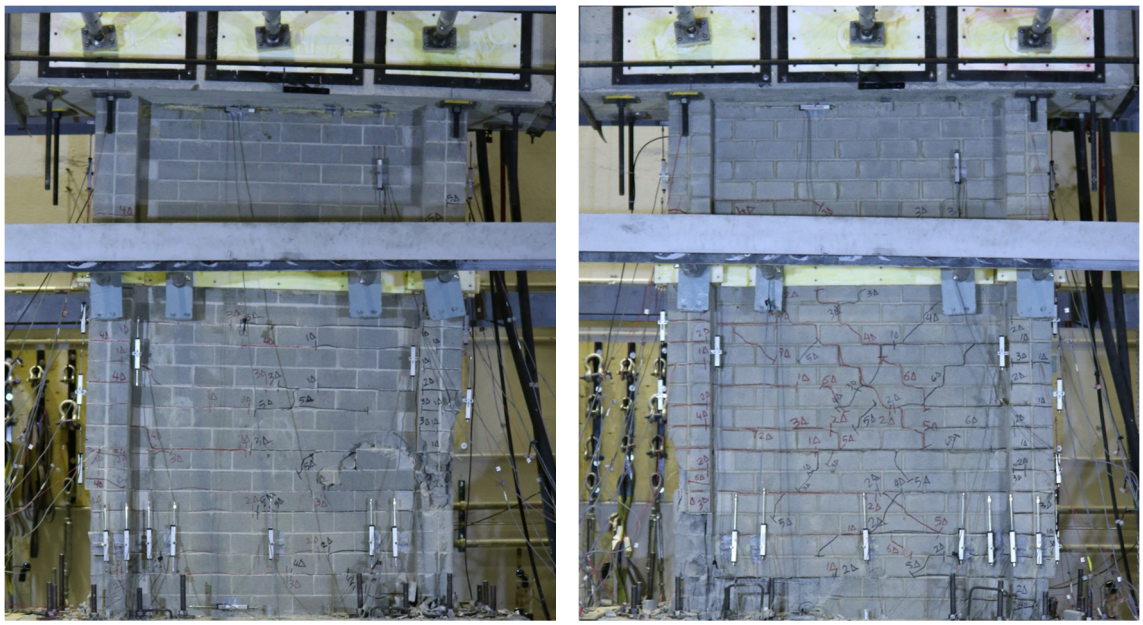

(a) (b)

Figure 6: Final damage state: (a) Wall W1; (b) Wall W2

Vertical cracking in boundary elements and toe-crushing was initiated at the peak of the displacement level of $6\Delta_y$ for W1 and $4\Delta_y$ for W2. As shown in Figure 6, both walls had most of the cracking and damage confined in the first floor, below the first level of out-of-plane support. This indicates that all plastic deformations occurred in the first floor and the tested heights were enough to represent the plastic hinge regions of the 12-story and 6-story walls. Furthermore, it is evident that the shear mechanism (diagonal and step cracks) was more dominant in the 6-story wall compared to the 12-story wall which had only a few diagonal shear cracks. Therefore, this observation further confirms the increased contribution of shear deformations in W2 and its influence on the cyclic strength degradation and the reduction in the strain-hardening in vertical rebars. Consequently, it demonstrates the capability of the utilized test setup in effectively capturing the changes in effective heights. Both walls failed in a ductile flexural mode characterized by buckling of vertical rebars in the boundary element combined with substantial crushing that extended to the wall web causing buckling of the first rebar in the web. In wall W1, this occurred during the second pull to the displacement level of $10\Delta_y$ which corresponds to a top of wall displacement equal to 56mm. Thus, wall W1 failed at a displacement-ductility factor (μ_Δ) of 10. Similarly, W2 reached its failure criteria during the second push to the displacement level of $8\Delta_y$ which corresponds to a top of wall displacement equal to 48mm. Therefore, wall W2 failed at a displacement-ductility factor (μ_Δ) of 8.

4 CONCLUSIONS

This study reports the preliminary results of quasi-static cyclic testing of two RCM shear walls with confined boundary elements. The two specimens had an almost identical cross-section, similar material properties and were tested under the same high level of axial pre-compression. However, the specimens differed in their shear span-to-depth ratio (M/Vd_v). The walls represented the expected plastic hinge panels of 12-story and 6-story RCM shear walls. The testing results demonstrated the capability of the presence of the confined boundary elements in improving the ductile response of mid- and high-rise RCM shear walls. The reduction in the shear span-to-depth ratio (from 8.8 to 4.4) resulted in a clear increase in the lateral stiffness

and the rate of stiffness degradation. Moreover, it increased the contribution of the shear mechanism to the overall structural response and limited the strain-hardening. There was a 9% reduction in the ratio between ultimate (Q_u) and yield (Q_y) loads when the wall's height was reduced from 12-story to 6-story. In addition, the 6-story wall had more distinct and rapid degradation in strength with the progressing loading cycles. W1 (12-story) had a hardening post-peak response whereas W2 (6-story) had a degrading post-peak response. Furthermore, the reduction in the shear span-to-depth ratio limited the wall ultimate displacement capacity. Nevertheless, the normalized response showed a similar overall response for the two specimens, confirming the limited influence of the changes in height compared to the influence of the cross-section.

ACKNOWLEDGEMENTS

The Authors acknowledge the support from the Natural Science and Engineering Research Council of Canada (NSERC), l'Association des Entrepreneurs en Maçonnerie du Québec (AEMQ), the Canadian Concrete Masonry Producers Association (CCMPA) and Canada Masonry Design Centre (CMDC).

REFERENCES

Ahmadi, F., Hernandez, J., Sherman, J., Kapoi, C., Klingner, R. E., and McLean, D. I. 2014. Seismic Performance of Cantilever-Reinforced Concrete Masonry Shear Walls. *Journal of Structural Engineering,* ASCE*,* **140** (9): 04014051.

"American Society for Testing and Materials (ASTM)." 2015. *Standard Test Methods for Sampling and Testing Concrete Masonry Units and Related Units, C140-15*. West Conshohocken, PA, USA.

Banting, B. and El-Dakhakhni, W. 2014. Seismic Performance Quantification of Reinforced Masonry Structural Walls with Boundary Elements. *Journal of Structural Engineering,* ASCE*,* **140** (5): 1–15.

Correa, M. R. S. 2016. A 20-Storey High Masonry Building in Brazil — Design Problems and Adopted Strategies. In *16th International Brick and Block Masonry Conference*, 623–28. Padova, Italy.

"Canadian Standard Association (CSA)." 2014. *CSA Standards on Concrete Masonry Units, A165-14*. Mississauga, Ontario, Canada.

"Canadian Standard Association (CSA)." 2014. *Design of Masonry Structures, S304-14*. Mississauga, Ontario, Canada.

Drysdale, R. G., and Hamid. A. A. 2005. *Masonry Structures Behaviour and Design*. Canadian e. Canada Masonry Design Centre, Mississauga, Ontario, Canada.

Federal Emergency Management Agency (FEMA). 2007. "FEMA 461, Interim Testing Protocols for Determining the Seismic Performance Characteristics of Structural and Nonstructural Components." *Prepared for the Federal Emergency Management Agency, Prepared by the Applied Technology Council, Washington D.C, USA.*

"National Building Code of Canada (NBCC)." Institute for Research in Construction, National Research Council of Canada." 2015. Ottawa, Ontario, Canada.

Shedid, M., El-Dakhakhni, W. and Drysdale, R. G. 2010. Alternative Strategies to Enhance the Seismic Performance of Reinforced Concrete-Block Shear Wall Systems. *Journal of Structural Engineering,* ASCE, **136** (6): 676–89.